Pis'ma v ZhETF, vol. 90, iss. 5, pp. 408 – 411

Unusually strong coherent response from grain-boundary Josephson network in polycrystalline $Pr_xY_{1-x}Ba_2Cu_3O_{7-\delta}$

V. A. G. Rivera[+], *S. Sergeenkov*[+], *C. Stari*[+*], *L. Jr. Cichetto*[+], *C. A. Cardoso*[+], *E. Marega*[∇], *F. M. Araujo-Moreira*[+]

[+] *Departamento de Física e Engenharia Física, Grupo de Materiais e Dispositivos, Centro Multidisciplinar para o Desenvolvimento de Materiais Cerâmicos, Universidade Federal de São Carlos, 13565-905 São Carlos, SP Brazil*

[*] *Instituto de Física, Facultad de Ingenieria, Julio Herrera y Reissig 565, C.C. 30, 11000, Montevideo, Uruguay*

[∇] *Instituto de Física, USP, 13560-970 São Carlos, SP, Brazil*

Submitted 23 June 2009
Resubmitted 23 July 2009

By applying a highly sensitive homemade AC susceptibility technique to $Pr_xY_{1-x}Ba_2Cu_3O_{7-\delta}$ polycrystals (with $x = 0.0$, 0.1 and 0.3), we observed very sharp Fraunhofer type low-field periodic oscillations of the real part of the AC susceptibility which were attributed to Josephson vortices penetrating intergranular regions of grain-boundary Josephson network in our samples. Assuming the Lorentz type distribution of single-junction contact areas, we were able to successfully fit the experimental data.

PACS: 74.25.Ha, 74.50.+r, 74.62.Dh

Introduction. It is well-known that important for large-scale applications properties of any realistic device based on Josephson effects require a very coherent response from many Josephson contacts comprising such a device (see, e.g., [1 – 8] and further references therein). Usually, due to inevitable distribution of critical currents and sizes of the individual junctions, a grain-boundary induced Josephson network in polycrystalline materials manifests itself in a rather incoherent way, making it virtually impossible for applications. That is why, ordered artificially prepared (hence more costly) Josephson junction arrays (JJAs) are used instead to achieve the expected performance [9 – 14].

In this Letter we report on unusually strong coherent response of grain-boundary Josephson network in our polycrystalline $Pr_xY_{1-x}Ba_2Cu_3O_{7-\delta}$ (PYBCO) samples which manifest itself through a clear Fraunhofer type magnetic field dependence of the measured AC susceptibility (more typical for ordered JJAs).

Results. High quality PYBCO bulk polycrystalline samples have been prepared by following a chemical route based on the sol-gel method [15]. The phase purity and the structural characteristics of our samples were confirmed by both scanning electron microscopy (SEM) and x-ray diffraction (XRD) along with the standard Rietveld analysis. The analysis of the XRD data (Fig.1) reveals that no secondary phases are present in our samples and that the peaks correspond to the orthorhombic structure with $YBa_2Cu_3O_{7-\delta}$ (YBCO) stoichiometric phase. The onset temperatures T_C (shown in Fig.3 for all studied samples) were independently confirmed via the resistivity, magnetization and AC susceptibility data, and well correlate with the values reported in the literature for polycrystalline samples with a similar composition [16, 17]. Fig.2 shows the SEM scan of grain-boundary morphology in the undoped YBCO

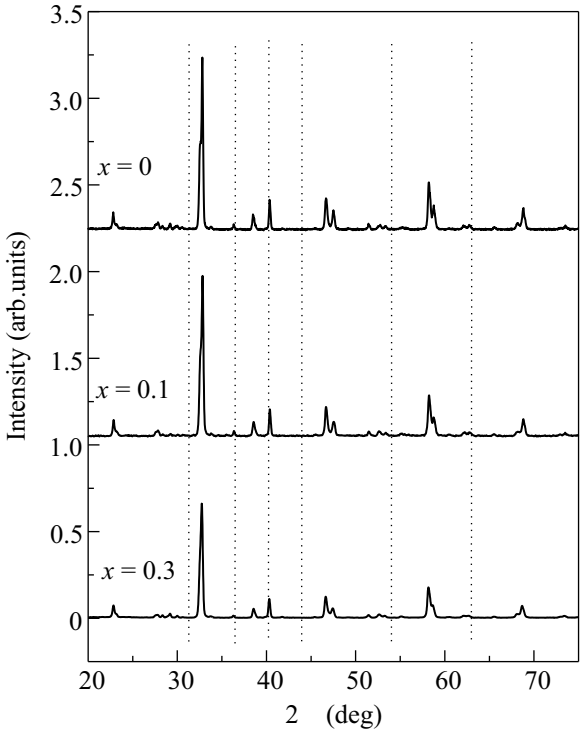

Fig.1. XRD patterns of $Pr_xY_{1-x}Ba_2Cu_3O_{7-\delta}$ samples

sample (with grains of different shape and average size of the order of $1\,\mu m$).

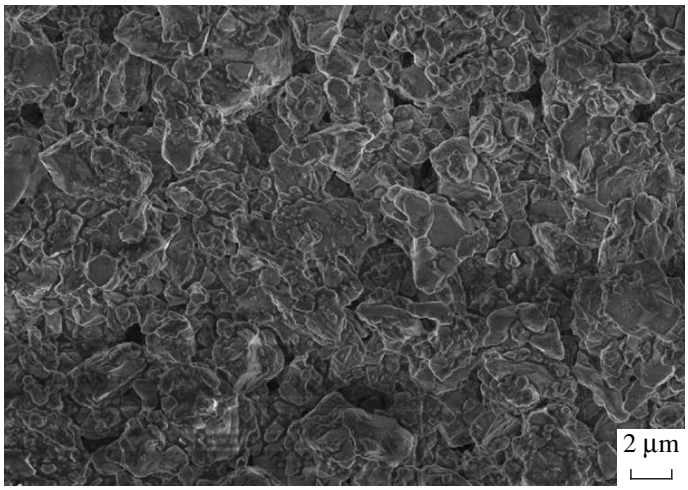

Fig.2. SEM scan photography of $YBa_2Cu_3O_{7-\delta}$

AC measurements were made by using a high-sensitivity homemade susceptometer based on the screening method and operating in the reflection configuration [9, 14]. The complex response $\chi_{ac} = \chi^{'} + i\chi^{''}$ was measured as a function of the AC field $h_{ac}(t) = h\cos(\omega t)$ (applied normally to the sample's surface with the amplitude $0.01\,\text{Oe} \leq h \leq 50\,\text{Oe}$ and frequency $1\,\text{kHz} \leq \omega \leq 30\,\text{kHz}$) taken at fixed temperature. The field dependence of the normalized real part of AC susceptibility $\Delta\chi^{'}(h) = \chi^{'}(h) - \chi^{'}(0)$ for different temperatures and Pr content is shown in Fig.3. As it is evident from this picture, there are two distinctive regions. Namely, above $h = 15\,\text{Oe}$ the curves exhibit almost linear dependence which can be attributed to establishment of the well-documented [18–21] Bean type critical state regime with $1 + 4\pi\chi_B^{'}(h) = 2h/J_C D$ where J_C is the field-independent critical current density and D the sample's thickness. On the other hand, below $h = 15\,\text{Oe}$, practically temperature-independent periodic oscillations are clearly seen. In what follows, we shall focus on explanation of this interesting phenomenon.

Discussion. To understand the observed behavior of $\Delta\chi^{'}(h)$, it is quite reasonable to assume that the low-field AC response in our samples is related to a Josephson network mediated intergranular contribution [22–24] $\chi_J^{'}(h)$. Notice, first of all, that the field oscillations manifest themselves in a rather narrow region between two characteristic Josephson fields: the lower critical field $h_{c1}^J = \Phi_0/2\pi\lambda_J^2$ and the upper critical field $h_{c2}^J = \Phi_0/2\pi\lambda_J d$. Here, $\lambda_J = \sqrt{\Phi_0/2\pi\mu_0 J_C d}$ is the Josephson penetration depth (which also defines the size of a Josephson vortex), and $d = 2\lambda_L + l \simeq 2\lambda_L$ is the width of a single contact with λ_L being the London penetration depth and l the thickness of the insulating layer. Based on the above critical fields, the flux penetration scenario can be described as follows. For $h < h_{c1}^J$, we have analog of the Meissner state for intergranular region (total screening of the applied field). When $h > h_{c1}^J$, field starts to penetrate into the intergranular region in the form of Josephson vortices (hence, h_{c1}^J is analog of the Abrikosov lower critical field $h_{c1}^A = \Phi_0/2\pi\lambda_L^2$). Since (unlike Abrikosov vortices) Josephson vortices are coreless, they will nucleate in the contact area $S = Ld$ (where L is the length of the contact) until their distribution becomes homogeneous. This process takes place for field region $h_{c2}^J > h > h_{c1}^J$ and manifests itself in the Fraunhofer type dependence of the Josephson current $I_J(h) = I_J(0)(\sin f/f)$ with $f = h/h_J$. The structure of the pattern is governed by the characteristic Josephson field $h_J = 2\pi S/\Phi_0$ which indicates how many fluxons penetrate the contact area S. At $h \simeq h_{c2}^J$, the Fraunhofer pattern practically disappears. More precisely, $I_J(h_{c2}^J) \ll I_J(0)$ (hence, h_{c2}^J indeed plays a role of the upper critical field for Josephson vortices). For $h_{c1}^A > h > h_{c2}^J$, we have a conventional Meissner state for the intragranular region (applied field still can not penetrate inside grains). The formation of the intragranular Abrikosov mixed state starts only for $h > h_{c1}^A$.

In order to clarify the origin of the discussed here effects, let us estimate the values of the above critical fields (and the corresponding depths). By relating the lower Josephson field $h_{c1}^J = \Phi_0/2\pi\lambda_J^2$ with the beginning of the observed oscillations (which is $h_{c1}^J \simeq 3.5\,\text{Oe}$ for pure YBCO sample), we obtain $\lambda_J \simeq 1\mu m$ for the size of the Josephson vortex. On the other hand, by relating the upper Josephson field $h_{c2}^J = \Phi_0/2\pi\lambda_J d$ with the end of oscillating behavior (which is $h_{c2}^J \simeq 15\,\text{Oe}$ for the same sample), we get $\lambda_L \simeq 100\,\text{nm}$ as a reasonable estimate of the London penetration depth in this material [16]. To account for the observed evolution of the Josephson fields with Pr concentration x, we recall [17] that in addition to the critical temperatures $T_C(x) \simeq T_C(0)(1-x)$, both the London depth $\lambda_L(x)$ and the critical current density $J_C(x)$ decrease upon doping. Namely, assuming that $\lambda_L(x) \simeq \lambda_L(0)(1-x)$ and $J_C(x) \simeq J_C(0)(1-x)$, we obtain $\lambda_J(x) \simeq \lambda_J(0)/(1-x)$, $h_{c1}^J(x) = \Phi_0/2\pi\lambda_J^2(x) \simeq h_{c1}^J(0)(1-x)^2$ and $h_{c2}^J(x) = \Phi_0/4\pi\lambda_J(x)\lambda_L(x) \simeq h_{c2}^J(0)$ for doping induced variation of the Josephson depth, lower and upper Josephson fields, respectively. Notice first of all that (in accord with our observations) the upper field does not change with Pr and has the same value ($h_{c2}^J \simeq 15\,\text{Oe}$) for all three samples. As for the lower field, according to the above

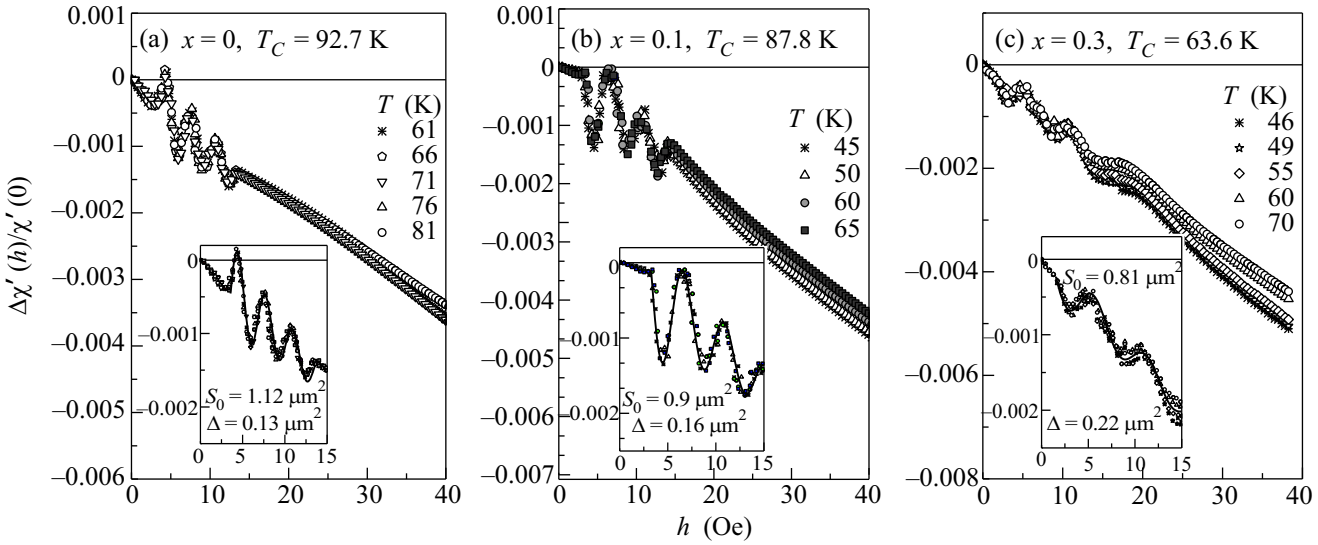

Fig.3. The magnetic field dependence of the normalized real part of AC susceptibility at different temperatures for samples with different Pr content x. Inset: the best fits (solid line) of the low-field region according to Eqs.(2)–(4)

simplified expressions, we have $h^J_{c1}(x=0) \simeq 3.5Oe$, $h^J_{c1}(x=0.1) \simeq 0.8h^J_{c1}(x=0) \simeq 2.8$ Oe, and $h^J_{c1}(x = 0.3) \simeq 0.49h^J_{c1}(x=0) \simeq 1.75$ Oe for $x=0$, $x=0.1$, and $x=0.3$, respectively. All these estimates are in good agreement with the observed onset of field oscillations (see Fig.3). Besides, the above x-dependence of the London penetration depth results in the following evolution of the contact area $S(x) \simeq S(0)(1-x)$ where $S(0) \simeq 2L\lambda_L(0)$. Now we can also estimate the value of this area for each of three samples by relating the number of trapped fluxons $n(x) = 2\pi hS(x)/\Phi_0$ with the number of the observed oscillation minima (seen in Fig.3) for the applied field span (lying between the lower and upper critical fields) $h \simeq h^J_{c2}(x) - h^J_{c1}(x)$. Namely, using $n(0)=4$, $n(0.1)=3$, and $n(0.3)=3$, we obtain $S(0) \simeq 1\,\mu$m^2, $S(0.1) \simeq 0.9\,\mu$m^2, and $S(0.3) \simeq 0.7\,\mu$m^2 for the estimates of contact areas in our three samples, which remarkably correlate with the above assumed doping dependence of $S(x)$. Moreover, the doping dependence of the London penetration depth $\lambda_L(x)$ also controls the evolution of the lower Abrikosov field, $h^A_{c1}(x) = h^A_{c1}(0)/(1-x)^2$ leading to the following estimates: $h^A_{c1}(0) \simeq 0.03$ T, $h^A_{c1}(0.1) \simeq 0.04$ T, and $h^A_{c1}(0.3) \simeq 0.06$ T. Therefore, given a markedly different values for Josephson and Abrikosov critical fields, we can safely assume that the discussed here phenomenon is strictly related to the Josephson physics. A pronounced Fraunhofer type form of the observed curves suggests a rather strong coherent response from many Josephson junctions comprising the grain-boundary network (despite some distribution in sizes of the individual junctions seen in Fig.2). To describe the observed phenomenon, we assume that intergranular contribution $\chi'_J(h)$ is related to AC field $h_{ac}(t) = h\cos(\omega t)$ induced modulation of the Josephson current $I_{ij}(t) = (2\pi/\Phi_0)J_{ij}\sin\theta_{ij}(t)$ (where J_{ij} is the Josephson energy) circulating in a closed plaquette (cluster) with a random distribution over contact areas S_{ij}. Each such cluster involves adjacent superconducting grains $i = 1, 2, ...N$ and $j = i+1$ with an effective phase difference $\theta_{ij}(t) = 2\pi S_{ij}h_{ac}(t)/\Phi_0$ across intergranular barriers [9, 23–26]. In turn, due to the Ampere's law, this circulating current $I_{ij}(t)$ produces a net magnetic moment [25, 26] $\mu(t) = \sum_{ij} I_{ij}(t)S_{ij}$, leading us to $\mathcal{H}(t) = \sum_{ij}\mathcal{H}_{ij}(t)$ for the total Hamiltonian describing the flux dynamics of a single plaquette with

$$\mathcal{H}_{ij}(t) = J_{ij}[1-\cos\theta_{ij}(t)] - \frac{2\pi}{\Phi_0}J_{ij}\sin\theta_{ij}(t)h_{ac}(t)S_{ij}, \tag{1}$$

where the second term is a Zeeman contribution $\mu(t)h_{ac}(t)$.

To obtain the experimentally observed intergranular contribution to the AC response, we assume (for simplicity) a Lorentz type distribution of the contact areas S_{ij} (around their mean values S_0 with the width Δ) of the form:

$$F(S_{ij}) = \frac{1}{\pi}\frac{\Delta}{(S_{ij}-S_0)^2+\Delta^2} \tag{2}$$

keeping in mind that the Josephson energy J_{ij} also depends on the contact area S_{ij} via a distance between grains r_{ij}. Namely, according to the conventional description of granular superconductors, $J_{ij} = J(0)\exp(-r_{ij}/2r_0)$, where r_0 is of the order of an

average grain size (radius). By using some geometrical arguments, it can be demonstrated that $S_{ij} \simeq$ $\simeq (r_{ij}/r_0)^2 S_0$ which results in the following explicit dependence of the Josephson energy on contact area, $J_{ij} =$ $= J(0)\exp(-\sqrt{S_{ij}/4S_0})$. Notice that this way we do not introduce any new fitting parameters (apart from the above mentioned S_0 and Δ).

Thus, the expression for the observed intergranular contribution to the AC susceptibility finally reads

$$\chi^{'}(h) = <\chi^{'}_J(h)>_S = \sum_{ij}\int_0^{S_m} dS_{ij}F(S_{ij})\chi^{'}_{ij}(h), \quad (3)$$

where

$$\chi^{'}_{ij}(h) = \frac{1}{2\pi V}\int_0^{2\pi} d(\omega t)\left[-\frac{\partial^2 \mathcal{H}_{ij}(t)}{\partial h^2_{ac}(t)}\right] = \quad (4)$$
$$= \chi_{ij}(0)\left[J_0(f_{ij}) - J_1(f_{ij})f_{ij}\right].$$

Here, $\chi_{ij}(0) = (2\pi S_{ij}/\Phi_0)^2 J_{ij}/V$ (V is the properly defined volume), J_n are the Bessel functions, and $f_{ij} =$ $= h/h^J_{ij}$, with $h^J_{ij} = \Phi_0/2\pi S_{ij}$ being a characteristic Josephson field (which is eventually responsible for the structure of the Fraunhofer pattern).

The best fits of the experimental data for the low-field region based on Eqs.(2)–(4) along with the values of two fitting parameters, S_0 and Δ, are shown as insets in Fig.3 (we assume $S_m = 2S_0$). In particular, for undoped YBCO sample, we found $S_0(0) = 1.12\,\mu\text{m}^2$ for the mean value of the contact area (which corresponds to the characteristic Josephson field $h_J(0) =$ $= \Phi_0/2\pi S_0(0) \simeq 2.8\,\text{Oe}$) and $\Delta(0) = 0.13\,\mu\text{m}^2$ for the contact area width distribution. The contact areas in the doped samples are found to be best fitted by the following set of parameters: $S_0(0.1) = 0.95\,\mu\text{m}^2$ (equivalent to $h_J(0.1) = \Phi_0/2\pi S_0(0.1) \simeq 3.3\,\text{Oe}$), $\Delta(0.1) = 0.16\,\mu\text{m}^2$, $S_0(0.3) = 0.81\,\mu\text{m}^2$ (equivalent to $h_J(0.3) = \Phi_0/2\pi S_0(0.3) \simeq 3.9\,\text{Oe}$), and $\Delta(0.3) =$ $= 0.22\,\mu\text{m}^2$. Notice that decreasing of $S_0(x)$ with x closely follows the earlier suggested doping dependence $S_0(x) \simeq S_0(0)(1-x)$, while the opposite behavior of the widths $\Delta(x)$ (increasing in doped samples) most likely reflects a random accumulation of Pr on grain boundaries, leading to a more broad distribution of the contact areas.

In summary, by using a highly sensitive home-made AC magnetic susceptibility technique, the magnetic flux penetration has been measured in high-quality $Pr_xY_{1-x}Ba_2Cu_3O_{7-\delta}$ polycrystals as a function of AC magnetic field for different temperatures and Pr doping. In addition to the conventional critical state behavior at higher fields, a clear manifestation of coherent intergranular response from Josephson vortices seen as a periodic Fraunhofer type dependence of the real part of AC susceptibility was observed at low magnetic fields.

The authors gratefully acknowledge Brazilian agencies CNPq, CAPES and FAPESP for financial support.

1. A. Barone and G. Paterno, *Physics and Applications of the Josephson Effect*, A Wiley-Interscience, New York, 1982.
2. V. Kaplunenko and G. M. Fischer, Supercond. Sci. Technol. **17**, S145 (2004).
3. T. G. Zhou, L. Fang, S. Li et al., IEEE Trans. Appl. Supercond. **17**, 586 (2007).
4. D. Koelle, R. Kleiner, F. Ludwig et al., Rev. Mod. Phys. **71**, 631 (1999).
5. H. Hilgenkamp and J. Mannhart, Rev. Mod. Phys. **74**, 485 (2002).
6. S. Sergeenkov, A. J. C. Lanfredi, and F.M. Araujo-Moreira, J. Appl. Phys. **100**, 123903 (2006).
7. D.-X. Chen, E. Pardo, A. Sanchez et al., J. Appl. Phys. **101**, 073905 (2007).
8. D. A. Balaev, A. A. Dubrovskiy, S. I. Popkov et al., J. Supercond. **21**, 243 (2008).
9. F. M. Araujo-Moreira, P. Barbara, A. Cawthorne, and C.J. Lobb, Phys. Rev. Lett. **78**, 4625 (1997).
10. R. S. Newrock, C. J. Lobb, U. Geigenmuller, and M. Octavio, Solid State Physics **54**, 263 (2000).
11. P. Martinoli and C. Leeman, J. Low Temp. Phys. **118**, 699 (2000).
12. S. M. Ishikaev, E. V. Matizen, V. V. Ryazanov, and V. A. Oboznov, JETP Lett. **76**, 160 (2002).
13. V. M. Krasnov, O. Ericsson, S. Intiso et al., Physica C **418**, 16 (2005).
14. F. M. Araujo-Moreira and S. Sergeenkov, Supercond. Sci. Technol. **21**, 045002 (2008).
15. P. N. Lisboa Filho, S. M. Zanetti, A. W. Mombru et al., Supercond. Sci. Technol. **14**, 522 (2001).
16. R. Khasanov, S. Strassle, K. Conder et al., Phys. Rev. B **77**, 104530 (2008).
17. V. A. G. Rivera, C. Stari, S. Sergeenkov et al., Phys. Lett. A **372**, 5089 (2008).
18. G. Pasquini, L. Civale, H. Lanza, and G. Nieva, Phys. Rev. B **59**, 9627 (1999).
19. J. H. Lee, Y. C. Kim, B. J. Kim, and D. Y. Jeong, Physica C **350**, 83 (2001).
20. A. Palau, T. Puig, and X. Obradors, J. Appl. Phys. **102**, 073911 (2007).
21. E. Bartolome, B. Bozzo, X. Granados et al., Supercond. Sci. Technol. **21**, 125002 (2008).
22. D.-X. Chen, E. Pardo, A. Sanchez, and E. Bartolome, Appl. Phys. Lett. **89**, 072501 (2006).
23. S. Sergeenkov and F. M. Araujo-Moreira, JETP Lett. **80**, 580 (2004).
24. S. Sergeenkov, Phys. Lett. A **372**, 2917 (2008).
25. C. Ebner and D. Stroud, Phys. Rev. B **31**, 165 (1985).
26. S. Sergeenkov and M. Ausloos, Phys. Rev. B **52**, 13619 (1995).